The Axially Modulated, Cusp-Injected, Large-Orbit Gyrotron Amplifier

W. Lawson, *Member, IEEE*, and W. W. Destler

Abstract— **We introduce a novel hybrid microwave amplifier that utilizes the axial bunching mechanism of klystrons in conjunction with the energy extraction mechanism of cyclotron resonance masers. A simple analytic model is used to show the viability of the device configuration and to explore limitations of the scheme. An example of an 11 GHz, 1 MW, fourth harmonic amplifier is presented. Adopting a single-particle approach, numerical simulations are used to demonstrate bunching in physical space and to estimate system efficiency. It is shown that this configuration enables the design of efficient, high harmonic devices over a wide range of parameters.**

I. Introduction

FUNDAMENTAL mode gyrotrons have proven to be reliable, efficient, high power (both peak and average) sources of microwave and millimeter wave radiation [1], [2]. Recent accomplishments include over 1 MW peak at 140 GHz for 2 μs [3] and 400 kW average at 140 GHz [4]. These devices have many potential applications including RF drive power for TeV linear supercolliders and other accelerators, millimeter wave and deep space radar, plasma heating in controlled thermonuclear research, and nonlinear spectroscopy of semiconductors and biological materials.

A major disadvantage of fundamental mode operation at high frequency is the requisite (large) applied magnetic field and the accompanying material bulk and/or power consumption. The idea of using rotating e-layers, i.e., large-orbit beams with zero guiding center radii, to reduce the magnetic field requirement via high-harmonic operation has received a fair amount of attention in the past few years both experimentally [5]-[15] and theoretically [16]-[23]. The required field is inversely proportional to the harmonic number, m, and thus the coil power is generally inversely proportional to m^2. The principle disadvantage of harmonic operation is that the efficiency typically decreases with increasing m. Recent experiments with short pulse, field emitter machines have produced moderate efficiencies $\leq$ 10% at high harmonics (10–20) with somewhat crude microwave diagnostics ($\pm$3 dB power uncertainty). Low power, microsecond pulse-length machines have produced comparable efficiencies at somewhat lower harmonics. Most of these systems have utilized a vane-type resonator to promote single-mode operation. The theoretical support has been dominated by linear growth rate calculations and the few large signal analyses make simplifying assumptions about the axial field variations (typically assumed to be sinusoidal). Consequently, these devices have not yet achieved their potential.

Recent attempts to improve efficiency have focused primarily on the application of linear tube energy recovery techniques to large-orbit geometry [24]. Unfortunately, this approach adds considerable complexity to the power supply and microwave output waveguide. Furthermore, there is a large capital cost associated with the collectors, insulators, and magnet system. Finally, this approach does nothing to improve the peak output power's dependence on beam voltage and current.

An alternate approach to enhanced efficiency is to remove, via beam pre-bunching, the particles which would gain energy by virtue of their location in phase space. This has received little attention in gyro-devices [15] but has been accomplished to varying degrees in linear devices by a number of techniques. The gigatron [25], [26] uses gated field-emitter silicon wafer cathodes to produce short current pulses. The lasertron [27], [28] utilizes photo-cathodes with high quantum efficiencies and picosecond laser pulses to gate emission. The klystrode [29] has a thermionic cathode with a control grid that is an integral part of a klystron-like cavity. An alternative to the gating approach is to use the ballistic bunching process of klystrons.

All four methods listed above are applicable to gyro-devices if we can convert axial bunching to azimuthal bunching. One technique that can be used to achieve this conversion involves passing the linear beam through a magnetic cusp. We will illustrate this process in Section II by examining the analytic model. In Section III, we will consider a specific example based on klystron bunching. Numerical techniques are used to estimate system performance. We summarize the results of this study in the final section.

II. Analytic Model

A schematic of this device is shown in Fig. 1. First consider only the dc motion of the beam by ignoring the presence of the microwave cavity. A simple thermionic diode with a thin, annular emitter strip is immersed in a uniform magnetic field. This diode produces a circular electron sheet in which each individual particle streams axially at a fixed radius and angle. Two long solenoids with oppositely directed currents (equal in magnitude) are separated by a thin ideal iron plate. At the plane of this junction, the electrons experience a rapid reversal in magnetic field direction which translates into a conversion of axial velocity to azimuthal velocity via the

Manuscript received August 27, 1993; revised February 10, 1994.

The authors are with the Electrical Engineering Department and Laboratory for Plasma Research, University of Maryland, College Park, MD 20742 USA.

IEEE Log Number 9404589D.

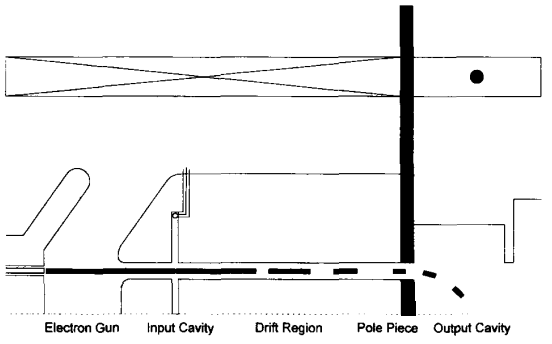

Fig. 1. A schematic of the axially-modulated, cusp-injected, large-orbit gyrotron.

Lorentz Force [30]. The net result is the production of a thin rotating annular sheet beam. The rotational velocity is simply equal to the product of the injection radius and the relativistic cyclotron frequency, $r\omega_{ce}$. The axial velocity of each particle downstream from the cusp is reduced by an amount that can easily be calculated from energy conservation. A spread in downstream axial velocity occurs due to the finite width of the emitter strip. The associated spread in canonical angular momentum results in a post-cusp perpendicular spread of $(\Delta v_\perp/v_{\perp_0})_{\rm RMS} = \Delta r/\sqrt{3}r_0$ where r_0 is the average cathode radius and $2\Delta r$ is the width of the strip. The corresponding axial velocity spread is approximately $\Delta v_z/v_{z_0} \approx \alpha^2 \Delta v_1/v_{\perp_0}$ where α is the average ratio of perpendicular to parallel velocity. This spread is one factor which limits efficiency and good performance demands fairly thin emitters. If the resulting cathode loading is a concern, beam power can be increased by using adiabatic compression [31].

Next, consider the requirements on a pre-bunched beam. In the ideal large-orbit system, the beam splits into m bunches and resonantly interacts with a circularly polarized TE_{mn} mode (though not required, typically $n = 1$). Constant phase of the EM fields is defined by the exponential term $\exp[j(\omega t - m\theta - k_z z)]$, where k_z is the axial wave number. The ideal beam has tightly-bunched electrons with the same general distribution. Near cutoff, where small-orbit gyrotrons typically operate, this requirement implies that the beam distribution involves m rigid rods which rotate in the azimuthal direction: $\theta = \theta_0 + \omega(t - t_0)/m$.

Consider an axially short cavity which is driven with two waveguides (or coaxial loops) that are separated by $90°/m$ in angle and 90° in (time) phase. At the proper frequency, this will generate a circularly polarized TM_{m10} wave in the cavity. A stream of electrons which passes through the cavity at a particular angle (say $\phi = 0°$) will experience an axial electric field which varies as $\cos(\omega t)$. Particles entering at $t = 0$ will be decelerated, while particles entering $1/2$ period later will be accelerated. Ballistic action will result in an axially bunched beamlet at some point downstream. Beamlets at other azimuthal angles will also bunch axially, but the bunches will be delayed or advanced in time due to the circularly polarized nature of the mode. In fact, if you observe the beam's variation in time at a fixed axial plane, the density will have m bunches that rotate at the drive frequency. When the electrons encounter the magnetic cusp, they begin to rotate at the cyclotron frequency. If $\omega = m\omega_{ce}$, the net effect is that the bunches line up and begin to rotate as required for cutoff operation. Choosing $\omega \neq m\omega_{ce}$ results in axial variations in the post-cusp bunch distribution as well.

To explore whether or not this method is a practical one, we need to consider the details of the bunching mechanism and cavity operation. The distance required between the microwave input cavity and the cusp can easily be estimated from single particle considerations (*i.e.* an Applegate Diagram [32]). If the cavity length is l, the peak field at the beam is E_b, and the original normalized beam velocity is v_0/c, then the maximum velocity kick is $\Delta v_m/c \approx eE_b l/mv_0 c$ where e and m are the usual electron charge magnitude and mass, respectively, and c is the speed of light. The distance in which a non-accelerated charge is overtaken by an accelerated one is $d = v_0^2/4f\Delta v_m$, where $f = \omega/2\pi$ is the microwave frequency. This distance can be shortened, and the bunching sharpened, by the introduction of passive bunching cavities between the drive cavity and the cusp. The spread in energy which results from the variation in electric field translates into perpendicular and parallel velocity spreads after the cusp. If the kick Δv is small, the approximate results below hold for each particle:

$$\frac{\Delta v_z}{v_{z_o}} = \left[1 + \alpha^2 + \alpha^2(\gamma_0^2 - 1)\right]\frac{\Delta v}{v_0},$$
$$\frac{\Delta v_\perp}{v_{\perp_0}} = -(\gamma_0^2 - 1)\frac{\Delta v}{v_0} \qquad (1)$$

where γ_0 is the relativistic mass factor. In the non-relativistic limit, the perpendicular spread is approximately zero and the parallel spread is $(\Delta v_z/v_{z_0})_{\rm RMS} \approx (1 + \alpha^2)\Delta v_m/\sqrt{2}v_0$. Consequently, except for the non-relativistic near-cutoff case, there is a trade-off between the bunching distance and the induced spread. It should be emphasized that these spread estimates neglect the effect of the cavity's magnetic field. In the simulations reported in the next section, it is often found that these fields typically modify each particle's canonical angular momentum in such a way as to decrease Δv_z significantly while increasing $\Delta v_\perp$ only moderately.

To first order, there is no net energy exchange between the beam and the cavity. Thus, drive power is required only to balance the wall losses at the prescribed field level. This power, which can be derived from standard EM textbooks [33], is given below for the TM_{m10} mode in terms of the peak electric field E_m:

$$P_{m1} = \pi x_{m1}\left[\frac{J'_m(x_{m1})}{J_m(x'_{m1})}\right]^2 \frac{a\delta_s}{1 + l/a}\frac{E_m^2}{2\eta_0} \qquad (2)$$

where J_m is the mth Bessel function of the first kind, x_{m1} and x'_{m1} are the first zeros of J_m and J'_m, respectively, η_0 is the impedance of free space, δ_S is the skin depth of the cavity at the operating frequency, and a is the cavity radius. Note that the required power depends only weakly on the cavity thickness l. (However, the velocity kick is proportional

to $E_m l$.) The outer radius is determined uniquely by the frequency: $a = cx_{m1}/\omega$. The radius where the electric field is a maximum is given by:

$$\frac{r_m}{a} = \frac{x'_{m1}}{x_{m1}} \approx \frac{1 + 0.808617m^{-2/3} + 0.072490m^{-4/3}}{1 + 1.855757m^{-2/3} + 1.033150m^{-4/3}} \quad (3)$$

where the approximation [34] is good to within 1% for all m. For harmonics between 4 and 10, the optimal radius is typically 70-81% of the wall radii. In general, r_m will be larger than the r_0 required for the field reversal. Of course, additional power can be used to compensate for the actual beam position, but there are several other ways to overcome this problem. First, a dielectric disk can be inserted into the cavity inside the beam radius (and possibly outside as well) to lower the optimal field location. Second, a cavity similar to the klystron's re-entrant cavity can be used to enhance the field at the beam. Finally, the drive cavity could be placed in the compression region (if the gun has one) where the average beam radius is larger.

Note that, with some difficulty, this cavity could be made an integral part of the cathode as in a klystrode. One problem is that the lower average velocity of the accelerating beam entails a thinner cavity. Furthermore, the cavity is in general more difficult to build and is complicated by its proximity to the thermionic cathode. Third, there is a net energy exchange between the cavity and the beam which requires additional microwave power. Finally, microwave coupling is complicated by the need for dc isolation. In parameter ranges where these obstacles can be overcome, there are several advantages to using the cavity to gate electrons. The advantages include: (1) the bunches are more tightly compressed (in general), (2) no drift region is required, and (3) there is virtually no spread in beam energy since the decelerated electrons are returned to the cathode.

For low power systems, the drift tube region would undoubtedly be a simple right-circular metal waveguide and the inner input cavity region could be supported by tungsten beam-intercepting pins [9], [11]. Higher power systems might have drift tube radii that permit the existence of EM modes at the drive frequency and may need to incorporate inner conductors or lossy dielectrics to isolate cavities. We note that dielectrics have been routinely inserted into some drift tubes and cavities with good success [36]. Furthermore, this device utilizes a linearly-streaming beam in the drift region and should be considerably more stable than pure gyro-amplifiers. The hardware inside the beam could, for example, be supported in a non-intercepting configuration by an Advanced Center-Post gun [37].

The output cavity for the axially-modulated systems should be in general no more complicated than the ones used in the usual large-orbit systems. In fact, they can typically have shorter axial lengths because of the decreased requirement for azimuthal bunching, often resulting in higher potential efficiencies. Further, the need for azimuthally periodic structures will be obviated for many configurations (*e.g.* relativistic systems) because the pre-bunched beam should suppress prospective competing modes.

TABLE I
SYSTEM PARAMETERS

1. Beam Parameters		
Voltage (kV)	100.	
Current (A)	25.	
Average radius (cm)	0.979	
Beam thickness (mm)	0.78	
Velocity ratio ($v\perp/v_z$)	0.0	(before cusp)
	2.0	(after ideal cusp)
2. Drive Cavity		
Drive frequency (GHz)	11.	
Azimuthal mode number	4.	
Radius (cm)	1.434	
Length (cm)	0.250	
3. Field Parameters		
Magnetic field (kG)	1.020	
Cavity - cusp spacing (cm)	25.	
Cusp width (cm)	0.500	
4. Extraction Cavity		
Radius (cm)	2.368	
Length (cm)	6.000	

III. DESIGN SIMULATION

As a concrete example, consider the design of an 11 GHz microwave system which is configured to extract energy from a 100 kV, 25 A beam at the 4th cyclotron harmonic. Traditionally, this system would require a long cavity with a slow wave structure (*e.g.* a vane resonator) to overcome the low growth rate. As will be shown below, pre-bunching allows the use of a fairly short right-circular cavity for energy extraction.

The nominal system parameters are shown in Table I. The beam can be derived from a standard electrode configuration followed by a magnetic compression region [23]. A specific design is not considered here because the gun parameters are fairly conservative (e.g. a cathode loading of 4 A/cm^2 and a compression ratio of 26). The table indicates the post-compression beam dimensions. The radial thickness corresponds to an ideal post-cusp velocity spread of $\Delta v_\perp = 2.31\%$.

The region in the drive cavity from $r = 0.81$ cm to $r = 1.15$ cm is assumed to be evacuated so that the beam has at least 1.3 mm clearance. The remainder of the cavity is filled with dielectric to minimize the outer radius. For the simulation we select a relative dielectric constant of $\varepsilon_r = 10$, which is near that of MgO. The input cavity length is arbitrarily picked so that the beam coupling factor [35] is greater than 0.95. No attempt has been made to optimize this length either for bunching or drive power considerations. The radial field variations for E_z and B_ϕ are shown in Fig. 2. The only other non-zero field (B_r) is proportional to E_z. The beam is located between the two peaks in E_z where the field is relatively large and flat. The latter feature helps to minimize the radial dependence of the optimal bunching length and is particularly important for finite width beams. Assuming a copper wall and a perfect dielectric, the field energy can be integrated to obtain a cold cavity input cavity quality factor of Q $\approx$ 3030. This value neglects beam loading but assumes critical coupling. When other non-ideal effects are accounted for, the quality factor and signal gain will decrease somewhat.

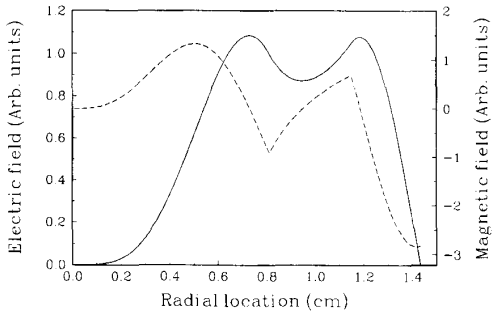

Fig. 2. The radial field profile profiles for the drive cavity. The solid line represents E_z and the dashed line represents B_ϕ. Note that dielectric-vacuum interfaces occur where the slope of B_ϕ is discontinuous.

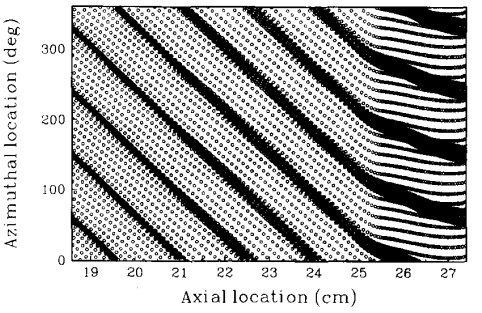

Fig. 3. The spatial distribution of electrons at one instant in time. The cusp is located between $z = 25$ cm and $z = 25.5$ cm.

The axial magnetic field is assumed to be constant on either side of the cusp. The magnitude is such that the cyclotron frequency (times 4) is detuned 13% from the drive frequency. This value is based on a crude efficiency optimization survey. The distance between the input cavity and cusp transition is chosen so that maximal bunching could be achieved with an input power of a few kilowatts. No attempt has been made to optimize the length. The transition is modeled with a linear variation in B_z. The transition width is readily achievable with the aid of one or more iron pole pieces.

A simple right-circular output cavity is considered. The standard sinusoidal axial field variation is assumed for computational purposes. No systematic length optimization has been attempted; the length is selected so that particles undergo approximately two revolutions inside the cavity.

Performance of this system is analyzed with a code that calculates single particle motion [31]. Convergence is checked by varying step size and particle number. Conservation of energy and canonical angular momentum are also checked in regions were there is only a static magnetic field. Numerical results are compared to analytic predictions wherever possible. Finally, start-oscillation thresholds are benchmarked against a standard gyrotron code [22]. Space-charge effects are neglected but are expected to be weak. The dc potential depression is ~5% in the output cavity and considerably less everywhere else. While ac space-charge will decrease axial bunching in the drift region, it should enhance azimuthal bunching in the output cavity. It remains for future work to determine under what conditions (if any) either effect will dominate performance. Most of the simulations are performed assuming an infinitesimally thin beam; the effect of beam thickness on efficiency is discussed toward the end of this section. The code is usually run in two stages. First, particles are followed through the input cavity and magnetic cusp. Then they are pushed through the output cavity to determine the steady-state energy exchange. The code assumes a particular electric field and calculates the optimal phase and output cavity quality factor required for energy balance. A linear magnetic field taper in the output cavity can be adjusted to optimize efficiency.

The bunching that results when a 4 kW TM_{410} signal is applied to the input cavity is illustrated in Fig. 3. A uniform azimuthal distribution of particles is initially "injected" into the code at $z = 0$ and regular time intervals. The figure indicates the downstream ϕ-z distribution of particles at a single instant in time. Each circle represents an individual electron. The magnetic cusp is situated between $z = 25$ cm and $z = 25.5$ cm. The bunches are fairly weak near $z = 19$ cm. At larger axial positions, the interbunch electrons become more widely separated and the bunch densities grow. As mentioned in the previous section, the azimuthal bunch location varies with axial position. Since the particles are linearly streaming (when $z < 25$ cm), at a constant axial plane the bunches will appear to rotate in a clockwise direction (larger ϕ). After the cusp, individual particles are also rotating in the clockwise direction and are traveling more slowly in the axial direction. In this example, $\omega > 4\omega_{ce}$, so the bunches still appear to drift back in ϕ with increasing z.

Immediately after the cusp, the beam has an average velocity ratio of $\alpha = 2.05$, a perpendicular velocity spread of 1.4%, a parallel velocity spread of 1.3%, and an energy spread of 3.55%. The average alpha is slightly higher than predicted due to the finite cusp width. The energy spread is nearly as predicted from the analytic model. However, $\Delta v_\perp$ is about twice the predicted value and Δv_z is nearly seven times smaller than expected. It can be shown that these discrepancies follow directly from the effects of the input cavity magnetic field.

The azimuthal r-ϕ particle distribution immediately following the cusp is indicated in Fig. 4(a). The numbers on the polar plot indicate the radial position in centimeters. The figure clearly indicates four well-formed azimuthal bunches. This is quantified in Fig. 4(b) where we plot the percentage of particles in 5° buckets for one azimuthal period. Nearly 73% of the particles are located within a 25° span and over 82% in a 45° span. Since the range of angles where the field is phased for energy extraction is 45° for an $m = 4$ mode, considerable energy extraction should be possible.

Fig. 5 reveals the dependence of efficiency on output cavity quality factor for a drive power of 4.2 kW. At each point, the magnetic field taper is adjusted to maximize efficiency. Optimal performance achieves 40.4% energy extraction and occurs when the peak electric field at the beam location is about 21 kV/cm in both cavities. The corresponding field maxima at the cavity walls are ~26 kV/cm in the input cavity

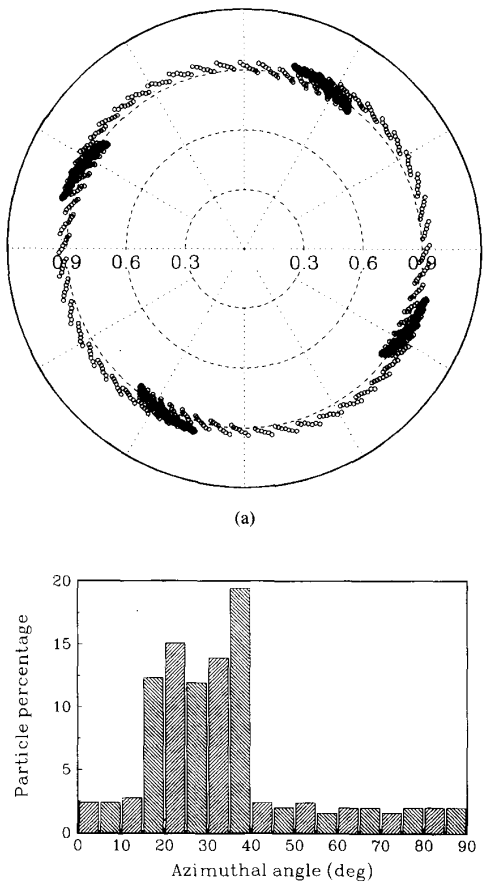

Fig. 4. The azimuthal distribution of particles at the entrance to the output cavity: (a) the r-ϕ distribution and (b) the azimuthal density over one azimuthal period.

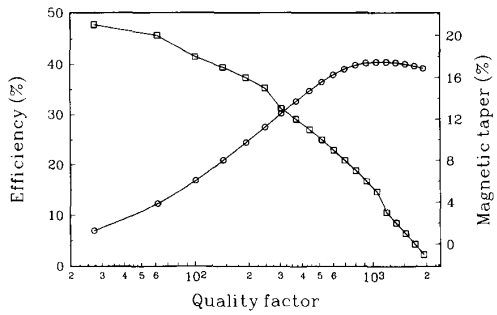

Fig. 5. The dependence of electronic efficiency on output cavity quality factor (P_{in} = 4.2 kW). The circles represent efficiency and the squares indicate taper strength.

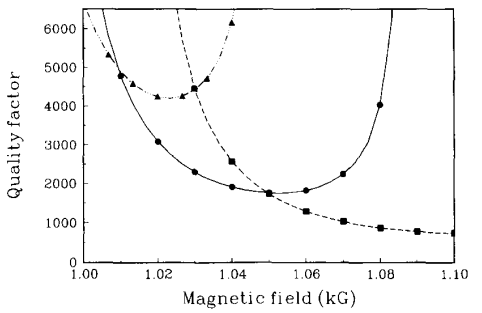

Fig. 6. The start-oscillation curve for the output cavity. The squares indicate the TE_{311} mode, the circles represent the TE_{411} mode, and the triangles denote the TE_{511} mode.

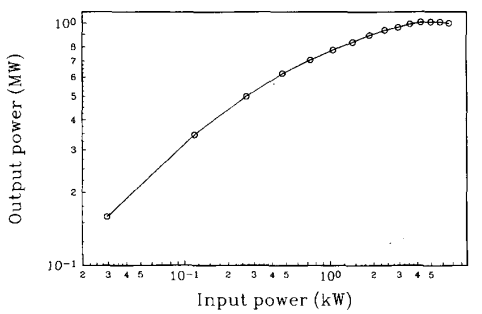

Fig. 7. Drive curve for an output cavity with Q = 1050.

and ~93 kV/cm in the output cavity. Both values are fairly conservative. The required cavity Q of 1050 is about 15 times smaller than the Q due to wall losses in a copper cavity, so over 93% of the microwave power can be extracted.

The quality factor required to achieve self-oscillation in the output cavity is shown in Fig. 6 as a function of (uniform) magnetic field. Curves are plotted for the TE_{411} mode and the two neighboring azimuthal modes. The minimum TE_{411} value of Q = 1760 at B_0 = 1.05 kG is considerably above the optimal value and amplifier operation should be feasible. The drive curve for the optimal configuration is shown in Fig. 7. The small signal gain is above 35 dB and the saturated gain is 23.7 dB.

The phase distribution of representative particles throughout their trajectories in the output cavity is shown in Fig. 8(a). For the azimuthal location, we actually plot ϕ-ϕ_0-ωt so that we can see the particle location relative to the EM wave fields. The phase is suitable for electron energy loss when $0 < \phi < 45°$ and $90° < \phi < 135°$. After the first centimeter, the majority of particles stay in the same bucket and drift only slowly back with respect to the fields. The corresponding energy loss as a function of axial location is given in Fig. 8(b). During the first centimeter the beam actually gains energy. Afterwards, the bulk of the particles give up energy so that the 40.4% efficiency is achieved by the time the particles leave the cavity.

The effect of beam thickness on efficiency at the optimal point has been examined briefly. When the thickness listed in Table I is modeled, the simulated post-cusp velocity spreads are $\Delta v_\perp = 2.57\%$ and $\Delta v_z = 9.28\%$. These values are close to what is expected from the combined effect of spreads due to beam thickness and velocity modulation. In spite of the relatively large axial velocity spread, the efficiency drops less than two points to $\eta = 38.8\%$.

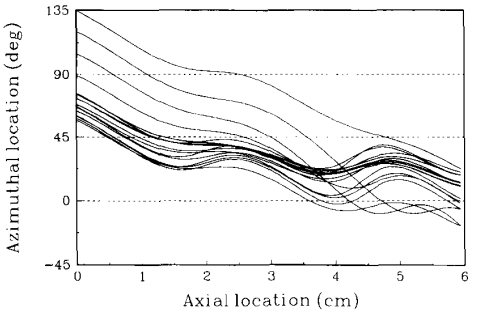

(a)

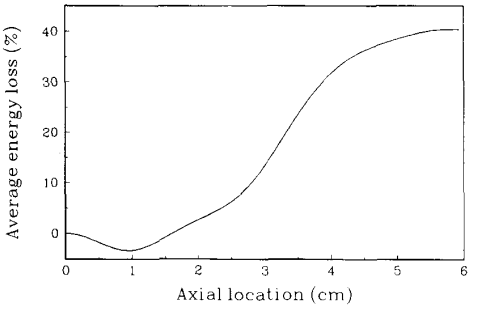

(b)

Fig. 8. Beam variations versus axial location in the output cavity: (a) representative electron trajectories relative to the EM wave's fields and (b) the beam's average energy loss.

IV. Discussion

The design expounded in this paper represents a new type of amplifier that is a hybrid between linear and gyro-devices. Its advantages over klystrons include the ability to use overmoded output cavities (low electric fields) and large annular beams. Its advantages over conventional gyroklystrons [36] include the ability to efficiently operate at high harmonics of the cyclotron frequency (low magnetic fields) and to produce bunching in a region where the beam is fairly stable to spurious oscillations. Given previous experimental results with high voltage, intense beam, high harmonic ($10 \leq m \leq 20$) systems, we expect that these axially modulated devices can be operated over a wide range of parameters.

The simulated efficiency of 40% is remarkable for several reasons. First, the example is intended only to demonstrate the principle of operation and very little effort has been put into maximizing efficiency. Second, it is highly unlikely that a non-prebunched, 100 kV large-orbit device can operate efficiently in a simple right circular cavity. Because the electric field near the required beam radius is increasing sharply (with r), particles which lose energy move to orbits where the interaction is weaker while particles that gain energy move to points with stronger interactions. The best efficiency we can simulate with a non-prebunched beam is $\eta = 17\%$ with a 10% field taper and an output cavity Q near 1600. It is unlikely that even this could be achieved because of competition from other azimuthal modes.

In the future we will work on an experimental verification of this concept. We will also look for higher efficiencies via the modeling of open-ended vane resonator structures and intermediate buncher cavities. Furthermore, we will investigate the effects of ac space-charge throughout the system. Finally, we will examine the potential to realize gating techniques which should actually produce superior bunches and even higher efficiencies.

Acknowledgment

The authors would like to thank M. K. E. Flaherty, P. E. Latham, H. W. Matthews and C. D. Striffler for many useful discussions.

References

[1] R. S. Symons and H. R. Jory, *Advances in Electronics and Electron Physics*, C. Marton, Ed. New York: Academic Press, 1981, vol. 55, ch. 1, p. 1.
[2] V. L. Granatstein, M. E. Read, and L. R. Barnett, *Infrared and Millimeter Waves*, K. Button, Ed. New York: Academic Press, 1981, vol. 5, ch. 5, p. 267.
[3] K. E. Kreischer, T. L. Grimm, W. C. Guss, A. W. Mobins, and R. J. Temkin, *Phys. Fluids B*, vol. 2, p. 640, 1990.
[4] K. Felch, C. Hess, H. Huey, E. Tongewaard, H. Jory, J. Neilson, R. Pendleton, and M. Tsirulnikov, in *Proc. SPIE*, vol. 1514, p. 315, 1990.
[5] W. W. Destler, D. W. Hudgings, M. J. Rhee, S. Kawasaki, and V. L. Granatstein, *J. Appl. Phys.*, vol. 48, p. 3291, 1977.
[6] W. W. Destler, H. Romero, C. D. Striffler, R. L. Weiler, and W. Namkung, *J. Appl. Phys.*, vol. 52, p. 2740, 1981.
[7] W. W. Destler, R. L. Weiler, and C. D. Striffler, *Appl. Phys. Lett.*, vol. 38, p. 570, 1981.
[8] W. W. Destler, R. Kulkarni, C. D. Striffler, and R. L. Weiler, *J. Appl. Phys.*, vol 54, p. 4152, 1983.
[9] W. Namkung, *Phys. Fluids*, vol. 27, p. 329, 1984.
[10] W. Lawson, W. W. Destler, and C. D. Striffler, *IEEE Trans. Plasma Sci.*, vol. 13, p. 44, 1985.
[11] E. Chojnacki, W. W. Destler, W. Lawson, and W. Namkung, *J. Appl. Phys.*, vol. 61, p. 1268, 1987.
[12] W. W. Destler, K. Irwin, W. Lawson, J. Rodgers, Z. Segalov, E. P. Scannell, and S. T. Spang, *J. Appl. Phys.*, vol. 66, p. 4089, 1989.
[13] K. Irwin, W. W. Destler, W. Lawson, J. Rodgers, E. P. Scannel, and S. T. Spang, *J. Appl. Phys.*, vol. 69, p. 627, 1991.
[14] K. K. Tiong and S. P. Kuo, *Int. J. Electron.*, vol. 70, p. 815, 1991.
[15] C. S. Kou, D. B. McDermott, N. C. Luhmann, Jr., and K. R. Chu, *IEEE Trans. Plasma Sci.*, vol. 18, p. 343, 1990.
[16] P. Sprangle, *J. Appl. Phys.*, vol. 47, p. 2935, 1976.
[17] H. S. Uhm and R. C. Davidson, *J. Appl. Phys.*, vol. 49, p. 593, 1978.
[18] Y. Y. Lau and L. R. Barnett, *Int. J. Infrared Millimeter Waves*, vol. 3, p. 619, 1982.
[19] K. R. Chu and D. Dialetis, *Int. J. Infrared Millimeter Waves*, vol. 5, p. 37, 1984.
[20] W. Lawson and C. D. Striffler, *Phys. Fluids*, vol. 28, p. 2868, 1985.
[21] W. Lawson and C. D. Striffler, *Phys. Fluids*, vol. 29, p. 1682, 1986.
[22] H. P. Bluem, P. E. Latham, W. Lawson, and C. D. Striffler, *IEEE Trans. Microwave Theory Tech.*, vol. 35, p. 946, 1987.
[23] W. Lawson and P. E. Latham, *J. Appl. Phys.*, vol. 61, p. 519, 1987.
[24] A. Singh, W. Lawson, D. Goutos, W. R. Hix, C. D. Striffler, V. L. Granatstein, and W. W. Destler, *Int. J. Electron.*, vol. 65, p. 351, 1988.
[25] H. M. Bizek, P. M. McIntyre, D. Raparia, and C. A. Swenson, *IEEE Trans. Plasma Sci.*, vol. 16, p. 258, 1988.
[26] E. G. Barasch, *et al.*, in *1992 LINAC Conference Proc.*, 1992, p. 519.
[27] C. K. Sinclair, SLAC-PUB-4111, 1986.
[28] M. Yoskioka, *Jap. J. Appl. Phys.*, vol. 28, p. 1079, 1989.
[29] D. H. Preist and M. B. Shrader, *IEEE*, vol. 70, p. 1318, 1982.
[30] M. J. Rhee and W. W. Destler, *Phys. Fluids*, vol. 17, p. 1574, 1974.
[31] W. W. Destler, E. Chojnacki, R. F. Heoberling, W. Lawson, A. Singh, and C. D. Striffler, *IEEE Trans. Plasma Sci.*, vol. 16, p. 71, 1988.
[32] Om. P. Ghandi, *Microwave Engineering and Applications*. New York: Pergamon Press, 1981, p. 285.
[33] J. D. Jackson, *Classical Electrodynamics*. New York: Wiley, 1975, p. 358.
[34] M. Abramowitz and I. A. Stegun, *Handbook of Mathematical Functions*. New York: Dover, 1965, p. 371.

[35] R. E. Collin, *Foundations for Microwave Engineering*. New York: McGraw-Hill, 1966, p. 468.
[36] W. Lawson, H. W. Matthews, M. K. E. Lee, J. P. Calame, J. Cheng, B. Hogan, P. E. Latham, V. L. Granatstein, and M. Reiser, *Phys. Rev. Lett.*, vol. 71, p. 456, 1993.
[37] G. P. Scheitrum, T. Bemis, T. A. Hargreaves, and L. Higgins, in *Proc. SPIE*, vol. 2104, p. 523, 1993.

Wes Lawson (S'84–M'85), for a photograph and biography see page 817 of this issue.

W. W. Destler, photograph and biography unavailable at time of publication.